Chula Med J. July - August 2025;69(4): 235 - 241 **DOI : 10.56808/2673-060X.**5579

Original article

Comparison of lung shunt fraction calculation using Tc-99m MAA planar and SPECT/CT imaging for Y-90 radioembolization

Nut Noipinit[a,*], Thunyaluk Sawatnatee[a], Benchamat Phromphao[a], Peangtawan Ratsameechot[b], Sutida Thiambandit[b], Tanawat Sontrapornpol[a]

[a]Department of Radiology, King Chulalongkorn Memorial Hospital, Thai Redcross Society, Bangkok, Thailand
[b]Department of Radiological Technology and Medical Physics, Faculty of Allied Health Sciences, Chulalongkorn University, Bangkok, Thailand

Abstract

Background: The evaluation of hepatopulmonary blood vessels using technetium-99m macroaggregated albumin (Tc-99m MAA) scintigraphy before radioembolization with yttrium-90 (Y-90) microspheres is a test employed to assess and prevent radiation pneumonitis. Moreover, the lung shunt fraction (LSF) was determined from planar and single-photon emission computed tomography/computed tomography (SPECT/CT) images. This study aimed to compare LSF calculations from Tc-99m MAA planar and SPECT/CT images for Y-90 radioembolization treatment of liver tumors.

Methods: A total of 64 patients (42 males, 22 females; mean age 64.0 ± 12.5 years) who underwent Tc-99m MAA scintigraphy between 2015 and 2022 were included in this study. The LSF was calculated using MIM software, with planar LSF derived from the geometric mean of lung and liver region of interest counts from anterior and posterior views, and SPECT/CT LSF from the volume of interest-based quantification. The two methods were compared using a paired *t*-test and Bland–Altman analysis. Intra-observer reliability was assessed using the coefficient of variation (%CV) from repeated measurements, while inter-observer reliability was evaluated using the intra-class correlation coefficient (ICC) from measurements by different investigators.

Results: The %CV for LSF remeasurements from planar and SPECT/CT images were 1.1% and 1.9%, respectively, indicating high intra-observer reliability. Inter-observer ICCs were 0.990 (planar) and 0.987 (SPECT/CT), thus confirming excellent agreement. Planar imaging yielded higher mean LSF values (7.0 ± 6.6%) than those of SPECT/CT (5.3 ± 4.6%), suggesting that planar methods tend to report higher LSF values.

Conclusion: This study demonstrates that LSF calculation using planar images yields significantly different results compared to those of SPECT/CT, with the LSF from planar images being slightly higher than those of SPECT/CT. Furthermore, LSF calculation using SPECT/CT combined with appropriate segmentation tools in MIM Encore software may provide more accurate results.

Keywords: LSF, planar, radioembolization, SPECT/CT, Tc-99m MAA.

According to global cancer statistics, in 2020, liver cancer ranked as the 6th most commonly diagnosed cancer and the 3rd leading cause of cancer-related deaths worldwide. Liver cancer is the most frequently diagnosed cancer in Thailand and the leading cause of cancer-related deaths. Moreover, hepatocellular carcinoma (HCC) accounts for 90.0% of all liver cancer cases. [1] Yttrium-90 (Y-90) microsphere radioembolization is a frequently employed technique in interventional radiology for patients with unresectable primary and secondary liver cancer. Radioembolization is a catheter-based therapy that delivers internal radiation to the tumors. [2] Y-90 is a beta-emitter used for radionuclide therapy with a maximum and average particle energy of 2.28 and 0.94 MeV, respectively. It can affect tumor cells up to a maximum range of 11 mm within the tissue. [3, 4] Before treatment, patients undergo mapping angiography and technetium-99m macroaggregated

*Correspondence to: Nut Noipinit, Department of Radiology, King Chulalongkorn Memorial Hospital, Thai Red Cross Society, Bangkok 10330, Thailand
E-mail: nut.no@chula.ac.th
Received: December 4, 2024
Revised: May 18, 2025
Accepted: June 25, 2025

albumin (Tc-99m MAA) scintigraphy. The information from these studies is used to minimize the risk of nontarget radiation injury to the gastrointestinal tract and lungs. [5, 6]

Radiation pneumonitis is a known complication of Y-90 radioembolization, and the risk thereof is related to the accidental delivery of radiation to the pulmonary tissue via hepatopulmonary shunting. Therefore, Tc-99m MAA scintigraphy is used to assess the degree of hepatopulmonary shunting. [7] Before treatment, patients undergo a Tc-99m MAA scan to obtain planar and SPECT/CT images, and these images are used to calculate the lung shunt fraction (LSF). The LSF is commonly calculated from planar images using the geometric mean (GM) formulation of counts obtained by defining the regions of interest (ROIs) of the liver and lungs in the anterior and posterior views. Single-photon emission computed tomography/computed tomography (SPECT/CT) is also often performed to qualitatively assess this with improved 3D imaging, which enables accurate definition of the liver and lungs. Furthermore, it is used to assess the distribution of particles with specific attention given to potential sites of extrahepatic deposition. [8-10] For Y-90 radioembolization, prescribed dose reductions are suggested for LSF > 10.0%. Moreover, a calculated LSF of > 20.0% or an LSF that results in an estimated lung radiation exposure of more than 30 Gy is considered a contraindication. [11-14]

Currently, the prediction of administered Y-90 activity at King Chulalongkorn Memorial Hospital (KCMH), Thai Red Cross Society, is performed by an interventional radiologist who estimates the LSF based on planar images. Therefore, this study aimed to compare LSF calculations from the Tc-99m MAA planar and SPECT/CT images for the Y-90 radioembolization treatment of liver tumors.

Materials and methods

Patients

This retrospective study was reviewed and approved by the Institutional Review Board and included patients diagnosed with histologically confirmed, unresectable primary or secondary liver malignancies who underwent Tc-99m MAA scintigraphy at KCMH between 2015 and 2022. Eligible patients were required to have complete planar and SPECT/CT imaging of both the liver and lungs, and those with incomplete image coverage were excluded from the analysis.

Image acquisition and reconstruction

Planar and SPECT/CT imaging in patients was performed using a Symbia Truepoint T6 (Siemens Healthineers, Germany) or Discovery NM/CT 670 (GE Healthcare, USA) system equipped with low-energy high-resolution collimators. Planar imaging of the chest and abdomen was performed within 1 h of Tc-99m MAA injection and included anterior and posterior views of the liver and lungs. The planar acquisition was set at a photopeak of 140 keV with a 20.0% window. After planar imaging, SPECT/CT images covering the whole liver and lungs were acquired using a dual-head gamma camera with a matrix size of 128 × 128 in the step-and-shoot mode, with 64 views (32 views per detector), 30 s per view, and 180° rotation per detector, which resulted in 360° coverage. Thereafter, ordered-subset expectation maximization, with 2 iterations and 10 subsets, and scatter correction were applied for image reconstruction.

Calculation of the LSF

Calculation of the LSF from the planar and SPECT/CT images was performed using MIM Encore software version 7.1.3 (MIM Software Inc., Cleveland, Ohio), as shown in **Figure 1**. In the planar images, the liver and lung ROIs were manually defined on the anterior and posterior views by two researchers and subsequently verified by a medical physicist with 7 years of experience. The LSF was calculated using the GM of the photon counts from each ROI in the anterior and posterior views. The LSF of the planar images can be calculated using equations (1) and (2) as follows:

$$\text{GM of lungs or liver} = \sqrt{\text{Anterior counts} \times \text{Posterior counts}} \quad (1)$$

$$\text{LSF} = \frac{GM_{Lungs}}{GM_{Lungs} + GM_{Liver}} \times 100 \quad (2)$$

For the SPECT/CT images, the liver and lung volumes of interest (VOIs) were performed using a semiautomated segmentation method. Automated segmentation of the liver and lungs was performed by creating a volumetric analysis using the axial, coronal, and sagittal images. These segmentations were manually adjusted by the same two researchers and verified by the same medical physicist to ensure accurate organ delineation. After segmentation, the LSF was calculated using the photon counts from each VOI with equation (3) as follows:

$$LSF = \frac{\text{Counts in lungs}}{\text{Counts in lungs} + \text{Counts in liver}} \times 100 \quad (3)$$

Inter- and intra-observer reliability

The intra-operator reliability was evaluated by randomly selecting patient imaging datasets. A single investigator delineated ROIs over the lungs and liver on planar images and VOIs on SPECT/CT images to calculate LSF values from both modalities. This process was repeated 10 times, and the coefficient of variation (%CV) of the resulting LSF values was calculated. A %CV of less than 5.0% was considered acceptable, indicating high intraoperator reliability. To assess interoperator reliability, imaging data from 10 randomly selected patients were used. Two independent investigators performed ROI and VOI delineation on planar and CT images, respectively, and the intraclass correlation coefficient (ICC) of the LSF values was calculated to evaluate the level of agreement between operators.

Statistical analysis

Statistical analysis was performed using SPSS 28.0 (SPSS Inc., Chicago, Illinois, USA) statistical software. Data are reported as the mean ± standard deviation (SD), and a paired *t*-test was used to compare the LSF values between the planar and SPECT/CT images, with a $P < 0.05$ considered significantly different. The agreement of LSF between the planar and SPECT/CT calculations was assessed using Bland-Altman plots.

Results

A total of 64 patients met the inclusion criteria, comprising 42 males and 22 females, with a mean age of 64.0 ± 12.5 years (range: 35–85 years). The relevant clinical and demographic characteristics are detailed in **Table 1.**

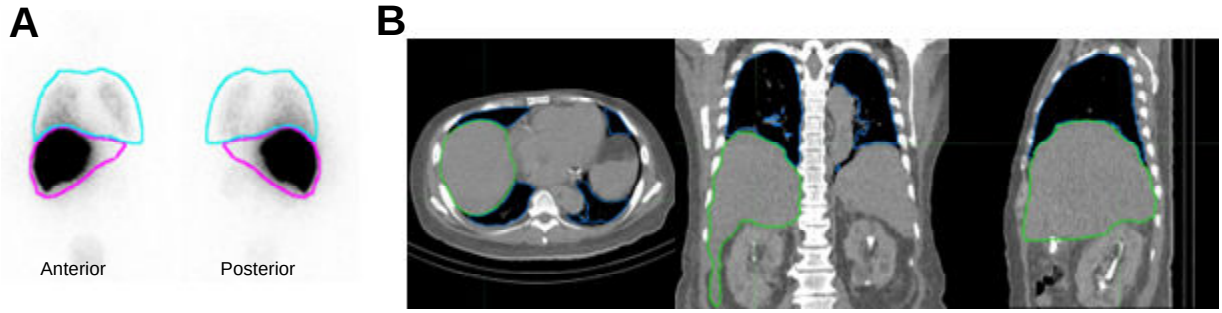

Figure 1. Manually drawing the ROIs of Tc-99m MAA from anterior and posterior views in planar images **(A)**. Semi-automated delineation of liver and lung regions using MIM Encore software in Tc-99m MAA SPECT/CT images **(B).**

Table 1 Clinical characteristics of patients

Characteristics	Overall
Patients (n = 64)	
Age (year)	64.0 ± 12.5
Range (year)	35 - 85
Gender	
Male	42 (65.6%)
Female	22 (34.4%)
Cancer type	
Hepatocellular carcinoma	58 (90.6%)
Colonic cancer	4 (4.3%)
Colorectal cancer	2 (3.1%)
Tc-99m MAA activity (MBq)	194.3 ± 59.9

Tc-99m MAA, technetium-99m macroaggregated albumin.

Inter- and intra-observer reliability

The %CV for the LSF remeasurements from the planar and SPECT/CT images were 1.1% and 1.9%, respectively, indicating high intra-observer reliability, as both were well below the 5% threshold. The ROI and VOI delineations by the same investigator exhibited no significant effect on the LSF values. The inter-operator reliability, assessed by ICC, was 0.990 for the planar and 0.987 for the SPECT/CT images, demonstrating excellent agreement between the two investigators, as both exceeded 0.90.

LSF from Tc-99m MAA imaging

According to the LSF results calculated by MIM software, the mean LSF values from the planar and SPECT/CT images were 7.0 ± 6.6 (range: 1.3–37.3) and 5.3 ± 4.6 (range: 1.6–29.5), respectively. The difference was statistically significant ($P < 0.001$). In 52 out of 64 cases (81.3%), the LSF from the planar images was higher than that from the SPECT/CT images, with a strong correlation between the two methods ($r^2 = 0.8861$), although the individual percent difference varied by case (**Figure 2**). In a small subgroup of cases (12 out of 64) with relatively low LSF from the planar images, SPECT/CT was found to yield higher LSF values (**Table 2).** The overall mean difference between the LSF from the planar and SPECT/CT images was 1.7, with a mean SD of 2.0. A Bland–Altman plot was constructed with the differences against their mean (**Figure 3).** The 95.0% limits of agreement of the differences were 7.1 and 3.6.

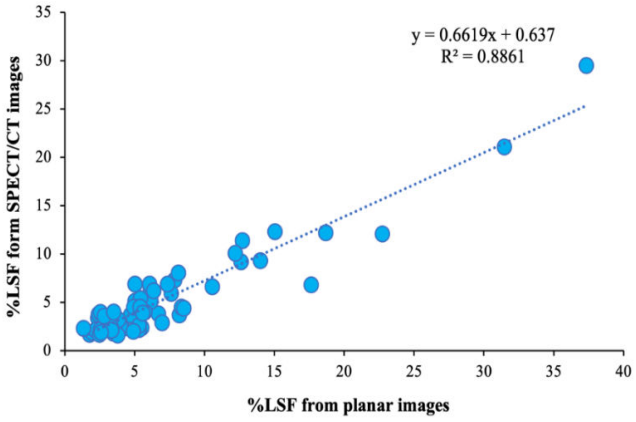

Figure 2. Linear correlation between LSF values obtained from planar and SPECT/CT images. LSF, lung shunt fraction; SPECT/CT, single-photon emission computed tomography/computed tomography.

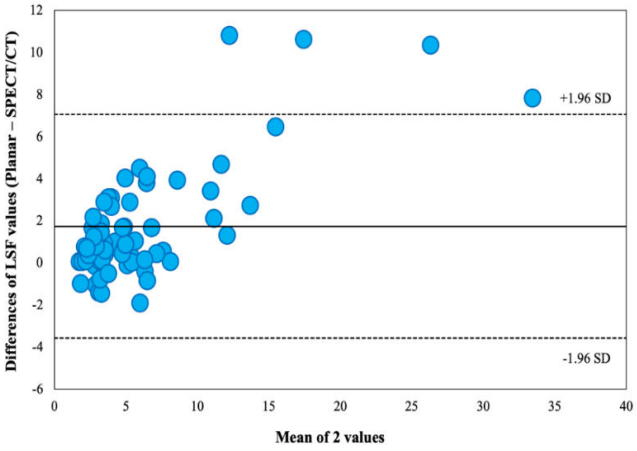

Figure 3. Bland–Altman plots of agreement and discrepancies between LSF obtained from planar and SPECT/CT images. LSF, lung shunt fraction; SPECT/CT, single-photon emission computed tomography/computed tomography.

Table 2. Comparison between planar and SPECT/CT for lung shunt fraction calculation.

Variables	LSF from planar images	LSF from SPECT/CT images
LSF < 10.0%	4.6 ± 1.9 (1.3–8.5)	4.0 ± 2.0 (1.6–9.3)
LSF 10.0% - 14.9%	12.4 ± 1.2 (10.6–14.0)	11.6 ± 0.9 (10.1–12.3)
LSF 15.0% - 19.9%	17.1 ± 1.9 (15.0–18.7)	–
LSF ≥ 20.0%	30.5 ± 7.4 (22.7–37.3)	25.3 ± 5.9 (21.1–29.5)
Mean LSF	7.0 ± 6.6 (1.3–37.3)	5.3 ± 4.6 (1.6–29.5)

LSF, lung shunt fraction; SPECT/CT, single-photon emission computed tomography/computed tomography.

Discussion

Because pneumonia is a notable complication for treating liver cancer with the localized radioactive administration of Y-90 microspheres, nuclear medicine imaging with Tc-99m MAA is required. This imaging is performed to assess and prevent radiation-induced pneumonitis that is caused by Y-90 microsphere treatment. Unlike other organs, such as the gastrointestinal tract, where the blockage of specific blood vessels can prevent the spread of radiation, the lungs cannot be protected in the same manner. [15] Therefore, this evaluation is essential for patient safety when planning their treatment. The assessment is based on the LSF, which can be calculated from planar and SPECT/CT images.

The results of this study demonstrated significant differences in the LSF values obtained from planar images compared to those obtained from SPECT/CT images **(Figure 4)**, which is consistent with findings from previous literature. [7, 16-18] The higher LSF observed in the planar images may be due to limitations in delineating the boundaries between the lung and liver in the planar images, leading to an overlap in the ROI. In 12 out of the 64 cases, the LSF obtained from the SPECT/CT images was higher than that from the planar images. This discrepancy may be attributed to the location of the liver lesions near the diaphragm and adjacent to the lungs, which could result in increased counts in the lung region. Furthermore, the lack of breathing control during image acquisition might have introduced respiratory movement-induced motion artifacts. These artifacts may have led to poor alignment between the SPECT and CT images, potentially resulting in an overestimation of the LSF in the SPECT/CT images compared to the actual value. [19, 20]

Furthermore, our study found that the LSF values obtained from the planar and SPECT/CT images were less than 10.0% in 53 cases, which allowed for the treatment with Y-90 microspheres as per the original treatment plan. For the two cases with LSF values between 10.0% and 14.9%, they could proceed with treatment, but with a recommended reduction in the radiation dose from the original plan. Meanwhile, in two cases with LSF values greater than 20.0%,

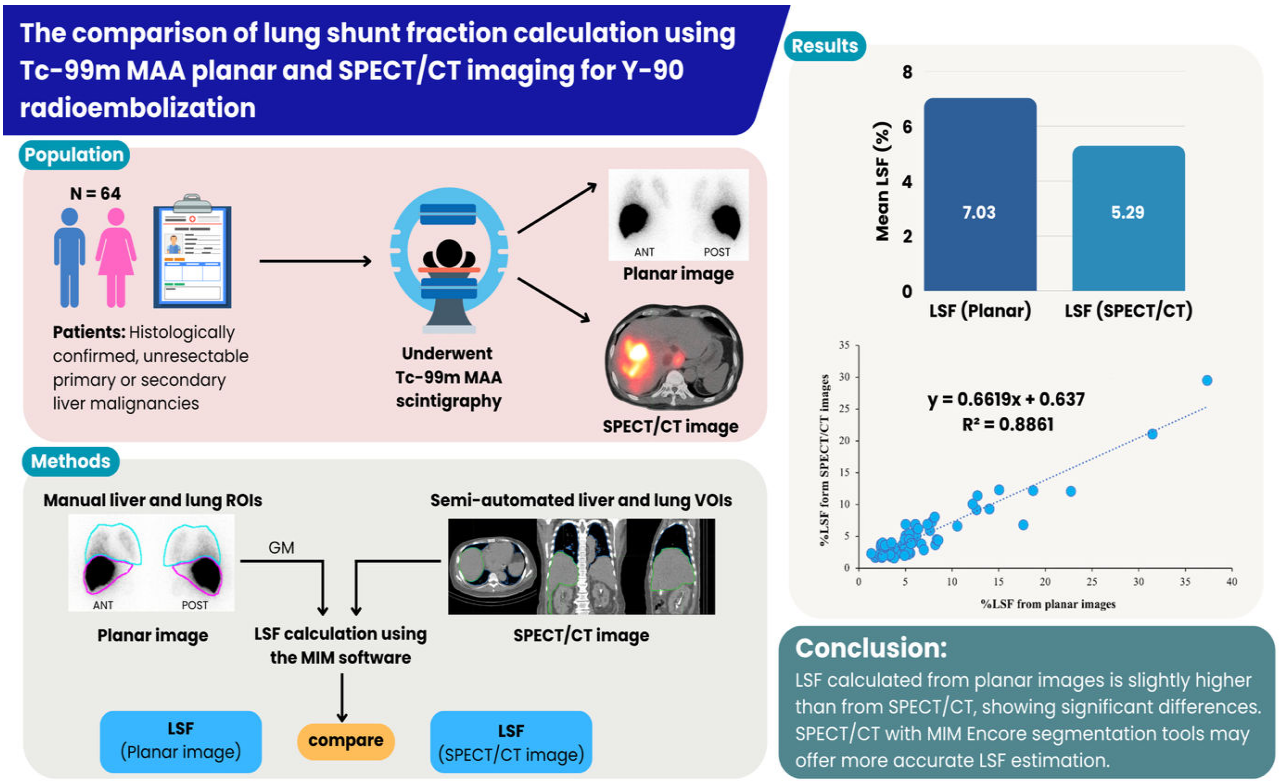

Figure 4. Summary of lung shunt fraction (LSF) comparison between Tc-99m MAA planar imaging and SPECT/CT in 64 patients with unresectable liver malignancies.

the treatment plan with Y-90 microspheres was rejected. In these two cases, the planar image LSF values were 31.5% and 37.3%, whereas the SPECT/CT image LSF values were 21.1% and 29.5%, respectively. In addition, there were seven cases where the LSF values obtained from planar imaging were greater than 10.0%, but the LSF values from SPECT/CT imaging were less than 10.0%. Among these, one patient had an LSF value of 22.7% from planar imaging and 12.1% from SPECT/CT imaging. Therefore, if the treatment decision was based on the LSF value obtained from SPECT/CT imaging, the patient might have had the opportunity to undergo liver cancer treatment using localized delivery of Y-90 microspheres. Regarding the outlier observed in the Bland–Altman plot, the LSF value derived from the planar images was higher than that obtained from the SPECT/CT images. This discrepancy could result in patients not receiving the full therapeutic dose of radiation or being denied treatment.

Conclusion

This study found that the LSF values obtained from planar images were significantly higher than those obtained from SPECT/CT images. This difference could have considerable clinical implications by reducing the number of patients requiring dose reduction or treatment cancellation. From our findings, it is recommended that the LSF obtained from SPECT/CT images should be considered in cases where the LSF from planar images is high. As SPECT/CT imaging provides 3D data with superior anatomical detail and more accurate organ delineation, it reduces organ overlap errors and improves measurement reliability. In addition, the appropriate segmentation tool in MIM Encore can further improve the accuracy of the LSF obtained from SPECT/CT images.

Acknowledgements

The authors would like to express their gratitude to all participants who were involved in this study.

Conflict of interest

All authors have completed and submitted the International Committee of Medical Journal Editors Uniform Disclosure Form for Potential Conflicts of Interest. All authors declare that they have no conflicts of interest.

Data sharing statement

All data generated or analyzed in the present study are included in the published article. Further details are available for noncommercial purposes from the corresponding author upon reasonable request.

References

1. Sung H, Ferlay J, Siegel RL, Laversanne M, Soerjomataram I, Jemal A, et al. Global cancer statistics 2020: GLOBOCAN estimates of incidence and mortality worldwide for 36 cancers in 185 countries. CA Cancer J Clin 2021;71:209–49.
2. Levillain H, Bagni O, Deroose CM, Dieudonné A, Gnesin S, Grosser OS, et al. International recommendations for personalised selective internal radiation therapy of primary and metastatic liver diseases with yttrium-90 resin microspheres. Eur J Nucl Med Mol Imaging 2021;48:1570–84.
3. Kim SP, Cohalan C, Kopek N, Enger SA. A guide to 90Y radioembolization and its dosimetry. Phys Med 2019;68:132–45
4. Weber M, Lam M, Chiesa C, Konijnenberg M, Cremonesi M, Flamen P, et al. EANM procedure guideline for the treatment of liver cancer and liver metastases with intra-arterial radioactive compounds. Eur J Nucl Med Mol Imaging 2022;49:1682–99.
5. Cremonesi M, Chiesa C, Strigari L, Ferrari M, Botta F, Guerriero F, et al. Radioembolization of hepatic lesions from a radiobiology and dosimetric perspective. Front Oncol 2014;4:210.
6. Wáng YX, De Baere T, Idée JM, Ballet S. Transcatheter embolization therapy in liver cancer: an update of clinical evidences. Chin J Cancer Res 2015;27:96–121.
7. Georgiou MF, Kuker RA, Studenski MT, Ahlman PP, Witte M, Portelance L. Lung shunt fraction calculation using Tc-99m MAA SPECT/CT imaging for Y-90 microsphere selective internal radiation therapy of liver tumors. EJNMMI Res 2021;11:96.
8. Torkian P, Ragulojan R, Woodhead GJ, D'Souza D, Flanagan S, Golzarian J, et al. Lung shunt fraction quantification methods in radioembolization: What you need to know. British J Radiol 2022;95:20220470.
9. Kao YH. Dosimetric theory for tumor-to-lung shunt fraction calculation in yttrium-90 radioembolization of noncirrhotic livers. Nucl Med Commun 2014;35:331-2.
10. Sundram FX, Buscombe JR. Selective internal radiation therapy for liver tumours. Clin Med (Lond) 2017;17:449–53.
11. Kallini JR, Gabr A, Hickey R, Kulik L, Desai K, Yang Y, et al. Indicators of lung shunt fraction determined by technetium-99 m macroaggregated albumin in patients with hepatocellular carcinoma. Cardiovasc Intervent Radiol 2017;40:1213–22.

12. Tong AKT, Kao YH, Too CW, Chin KFW, Ng DCE, Chow PKH. Yttrium-90 hepatic radioembolization: clinical review and current techniques in interventional radiology and personalized dosimetry. Br J Radiol 2016;89: 20150943.
13. Narsinh KH, Buskirk MV, Kennedy AS, Suhail M, Alsaikhan N, Hoh CK, et al. Hepatopulmonary shunting: A prognostic indicator of survival in patients with metastatic colorectal adenocarcinoma treated with 90Y radioembolization. Radiology 2016;282: 281–8.
14. Noipinit N, Sukprakun C, Siricharoen P, Khamwan K. Comparison of absorbed doses to the tumoral and non-tumoral liver in HCC patients undergoing 99mTc-MAA and 90Y-microspheres radioembolization. Ann Nucl Med 2023;38:210–8.
15. Leung TW, Lau WY, HO SK, Ward SC, Chow JH, Chan MS, et al. Radiation pneumonitis after selective internal radiation treatment with intraarterial 90yttrium-microspheres for inoperable hepatic tumors. Int J Radiat Oncol Biol Phys 1995;33:919–24.
16. Allred JD, Niedbala J, Mikell JK, Owen D, Frey KA, Dewaraja YK. The value of 99mTc-MAA SPECT/CT for lung shunt estimation in 90Y radioembolization: a phantom and patient study. EJNMMI Res 2018;8:50.
17. Kennedy A, Nag S, Salem R, Murthy R, McEwan AJ, Nutting C, et al. Recommendations for radioembolization of hepatic malignancies using yttrium-90 microsphere brachytherapy: a consensus panel report from the radioembolization brachytherapy oncology consortium. Int J Radiat Oncol Biol Phys 2007;68:13–23.
18. Struycken L, Patel M, Kuo P, Hennemeyer C, Woodhead G, McGregor H. Clinical and dosimetric implications of calculating lung shunt fraction for hepatic 90Y radioembolization using SPECT/CT versus planar scintigraphy. AJR Am J Roentgenol 2022;218:728–37.
19. Dittmann H, Kopp D, Kupferschlaeger J, Feil D, Groezinger G, Syha R, et al. A prospective study of quantitative spect/ct for evaluation of lung shunt fraction before sirt of liver tumors. J Nucl Med 2018;59:1366–72.
20. Gill H, Hiller J. Systematic review of lung shunt fraction quantification comparing SPECT/CT and planar scintigraphy for yttrium 90 radioembolization planning. Clin Transl Imaging 2021;9:181–8.